

**PEDESTAL CRATERS ON MARS: DISTRIBUTION, CHARACTERISTICS, AND IMPLICATIONS FOR AMAZONIAN CLIMATE CHANGE.** S. J. Kadish<sup>1</sup>, J. W. Head<sup>1</sup> and N. G. Barlow<sup>2</sup>. <sup>1</sup>Department of Geological Sciences, Brown University, Providence, RI 02912 USA (Seth\_Kadish@Brown.edu), <sup>2</sup>Department of Physics and Astronomy, Northern Arizona University, NAU Box 6010, Flagstaff, AZ 86011.

**Introduction:** Pedestal craters (Pd) (Figs. 1-2) are a subclass of impact craters on Mars [1] characterized by a crater perched near the center of a pedestal (mesa or plateau) that is surrounded by an often-circular, outward-facing scarp; the scarp is typically several crater diameters from the rim crest (Figs. 1-2), and tens to over 100 meters above the surrounding plains. First recognized in Mariner 9 data [2], Pd have been interpreted to form by armoring of the substrate during the impact event, usually by an ejecta covering [e.g., 3]. More recent hypotheses include increased ejecta mobilization caused by volatile substrates [4], distal impact-melt-rich veneers [5], and/or an atmospheric blast/thermal effect [6]. Following armoring, a marginal scarp is created by preferential erosion of the substrate surrounding the armored region, most commonly thought to involve eolian removal of fine-grained, non-armored material [e.g., 3]. The preferential distribution of Pd at latitudes above about 40° [7-9] (e.g., Fig. 3), together with an increased understanding of the role of redistribution of ice and dust during periods of climate change [e.g., 10-11] have led many researchers to suspect that the substrate might have been volatile-rich [8-9, 12-14]. Specifically, some [e.g., 8-9] have called on models of impact into volatile-rich targets to produce Pd during times of higher obliquity, when mid- to high-latitude substrates were characterized by thick deposits of snow and ice; return to lower obliquities would cause migration of regional ice and snow deposits back to the poles [e.g., 15], and sublimation of a thick regional volatile unit, except below the protective cover of pedestal craters. Thus, this model predicts that thick deposits of snow and ice should underlie Pd. Here we report on the results of a major study using new image and altimetry data that is designed to document and characterize pedestal craters on Mars equatorward of ~60° N and S latitude [8-9] in order to test these hypotheses for the origin of pedestal craters.

**The Analysis:** In this study we used new THEMIS VIS and IR image data to determine the distribution of all Pd with diameters >0.7 km between ~60°N and S latitude (between the red lines in Fig. 3). We located all Pd in this range and analyzed their characteristics, including size, lobateness ( $\Gamma$ ; a measure of pedestal margin sinuosity [8-9]), and ejecta mobility (EM; a measure of the extent of the pedestal compared to the crater diameter [8-9]). We located and measured 2422 Pd and their areal distribution is shown in Fig. 3 (between ~63°N and S latitude).

**Global Distribution:** Pd are not distributed randomly on Mars (Fig. 3). In the northern hemisphere, Pd are observed almost exclusively above 33°N, with the majority between 45° and 60°N latitude. Pd are not evenly distributed in this band; highest concentrations exist in Utopia Planitia and E of Acidalia Planitia, and there is a paucity in Tempe Terra. In the southern hemisphere Pd are less abundant, occur almost exclusively poleward of 40°S, and are concentrated in the south circum-Hellas region, particularly to the SW of Hellas. There is a dearth of Pd equatorward of ~40° N-S latitudes except in one area just W of Tharsis (0°-15°N; 125°-170°W) associated with the Medusae Fossae Formation (MFF) [14]. The general

distribution of Pd is clearly latitude-dependent and similar to the latitudinal distribution of 1) ice currently in the substrate [16-17], 2) surface roughness data interpreted to mean that the subjacent topography has been smoothed by emplacement of a meters to tens of meters thick mantle [18]; 3) a host of geomorphic features (e.g., ice-rich mantle, polygons, viscous flow features, dissected terrain) interpreted to represent the deposits from a recent ice age [11, 19], and 4) a wide range of ice-related features interpreted to represent Amazonian-aged deposition of ice and snow driven by climate change [20]. Furthermore, the outlier of Pd distribution in the near-equatorial MFF is consistent with interpretation of this area as previously ice-rich [14, 21-22]; Pd here, however, have very unusual attributes.

**Attributes of Pedestal Craters:** Crater diameters at the center of the pedestals in this study area are generally <5 km; the mean is <2 km. Pd crater diameters tend to increase toward the equator (except in the MFF). The lobateness ( $\Gamma$ ) ranges from ~1-2.5 with a mode slightly over 1; a value of 1 is perfectly circular, while higher values correspond to greater sinuosity. Most other types of fresh martian impact craters have distinctly higher marginal sinuosity [12,23]. The distinctive circularity of Pd plateaus ( $\Gamma$  values near unity; Fig. 1) favors an interpretation of the origin of armoring from symmetrical atmospheric blast/thermal effects [6], rather than effects related solely to ejecta armoring. Furthermore,  $\Gamma$  values near unity also favor modification of the pedestal margin by sublimation rather than eolian deflation, as eolian erosion would be influenced by and show the effects of prevailing wind directions. EM values are the ratio of pedestal diameter to crater diameter. EM values range from 1.2 to 13; mean values are ~3.7 at N latitudes and ~3.8 at S latitudes [12,23]. Pd crater EM values are the highest for any martian crater type [12]. These very high EM values are consistent with ejecta armoring and symmetrical atmospheric blast/thermal effects [e.g., 4-6] armoring the outer reaches of the pedestal. Together these would tend to influence the substrate to greater radial distances than ejecta alone. Furthermore, the volatile-rich nature of an ice-dust substrate could significantly improve the sintering and armoring efficiency of atmospheric blast/thermal effects associated with the impact [5-6]. Pd plateaus are typically ~50 m above the surrounding substrate. Plateaus associated with Pd with pitted margins [24] are higher, generally closer to ~100 m; some MFF plateaus are up to 200 m.

**Marginal Pits in Pedestal Craters:** Pedestal craters with marginal pits are a newly identified crater morphology in which numerous pits occur along or outline the marginal scarp of a pedestal crater [24]. The pits have a typical depth of ~20 m; Pd craters containing scarp pits identified thus far occur poleward of 50°N, between ~80°E and 160°E in Utopia Planitia (blue dots in Fig. 3). The crater ejecta deposit surface (top of the Pd) is perched several tens of meters (up to about 100 m) above the surrounding terrain, somewhat higher than a typical Pd crater. At the Pd plateau edge, the marginal scarp slopes down to the surrounding terrain, except where it is interrupted by a pit. We interpret these pits as sublimation pits in the scarps surrounding the pedestal craters. This interpretation provides direct evidence

that this class of Pd is underlain by ice and snow deposits, and suggests that other smaller Pd may also contain snow and ice.

**Discussion and Conclusions:** On the basis of these analyses, we find that: **1)** The distribution of pedestal craters is non-random and highly correlated with many climate indicators consistent with the presence of an ice cover at these latitudes in the Amazonian. **2)** The characteristics of pedestal craters with pitted margins [24] strongly support the current presence of volatiles below the armored surfaces of the Pd plateaus. **3)** The basic EM and  $\Gamma$  values are consistent with a combination of proximal crater ejecta armoring and distal symmetrical atmospheric blast/thermal effects [4-6] of an impact into a very volatile-rich substrate [e.g., 11]. **4)** The small size-range of distinctive pedestal craters suggests a delicate balance between crater size and the formation of this class of crater; ejecta from larger craters may overwhelm the volatile substrate layer. Volatiles buried beneath the interior of the ejecta of the larger craters could help to explain the anomalously high crater ejecta volumes (relative to crater volumes) observed at high N latitudes [25]. **5)** Our observations are consistent with pedestal crater formation being the result of impact into a target substrate consisting of a volatile-rich dust/snow/ice layer tens to hundreds of meters thick, overlying a dominantly silicate regolith; in the cratering event, ejecta armors the proximal region, and atmospheric blast/thermal effects sinter and armor the distal regions. Subsequent to formation of the crater, climate change [e.g., 20] causes the sublimation, lateral migration, and loss of the volatile-rich dust/snow/ice layer, lowering the regional surface down to the underlying silicate-rich regolith, and leaving a generally circular pedestal at the edges of the armored plateau surrounding the impact crater. Evidence of distinctive sublimation pits surrounding the margins of some of the largest Pd craters [24] strongly suggests that this processes is continuing at present. **6)** These data imply that during the Amazonian, significant climate change occurred causing deposition of

decameters-thick, latitude-dependent, ice-rich mantles. These Pd deposits not only represent a distinctive, accessible, probably layered record of Amazonian climate history, but they also signify that a significant amount of volatiles was removed from the active Amazonian water cycle and sequestered, adding further evidence of temporal sequestration of ice as a function of time in the Amazonian [20].

We are currently: 1) assessing regional variations in the properties of Pd in order to understand the distribution of ancient volatile-rich layers, 2) assessing the size-frequency distribution of Pd to understand the timing of these latitude-dependent volatile-rich layers, 3) targeting prominent Pd with the SHARAD radar instrument [26] in order to test for the presence and structure of candidate volatile-rich deposits, and 4) examining the relationships of these craters to larger craters in the same areas to assess the link between small and large crater morphology [1,4] and the possible presence of volatile-rich material under the larger crater ejecta deposits [27].

**References:** [1] N. Barlow et al. (2000) *JGR* 105, 26733. [2] J. McCauley (1973) *JGR* 78, 4123. [3] R. Arvidson (1976) *Icarus* 27, 503. [4] G. Osinski (2006) *MAPS* 41, 1571. [5] P. Schultz and J. Mustard (2004) *JGR* 109, E01001. [6] K. Wrobel et al. (2006) *MAPS* 41, 1539. [7] P. Mougini-Mark (1979) *JGR* 84, 8011. [8] S. Kadish and N. Barlow (2006) *LPSC* 37 #1254. [9] S. Kadish and N. Barlow (2007) *B-V* 46 #31. [10] B. Jakosky et al. (1995) *JGR* 100, 1579. [11] J. Head et al. (2003) *Nature* 426, 797. [12] N. Barlow (2005) *RVAMIC* #3041. [13] J. Head and R. Roth (1976) *LSI* 50-52. [14] P. Schultz and Lutz (1988) *Icarus* 73, 91. [15] B. Levrard et al. (2004) *Nature* 431, 1072. [16] W. Feldman et al. (2002) *Nature* 297, 75. [17] W. Boynton et al. (2002) *Nature* 297, 81. [18] M. Kreslavsky and J. Head (2000) *JGR* 105, 26695. [19] J. Mustard et al. (2001) *Nature* 412, 411. [20] J. Head and D. Marchant (2008) *LPSC* 39 this volume. [21] J. Head & M. Kreslavsky (2004) *LPSC* 35 #1635. [22] T. Watters et al. (2007) *Science* 318, 1125. [23] N. Barlow (2005) *RVAMIC* #3032. [24] S. Kadish et al. (2008) *LPSC* 39 this volume. [25] J. Garvin et al. (2000) *Icarus* 144, 329. [26] R. Phillips et al. (2007) *AGU Fall Mtg*, P14B-02. [27] B. Black and S. Stewart (2005) *RVAMIC* #3044; (2007) *JGR* in press.

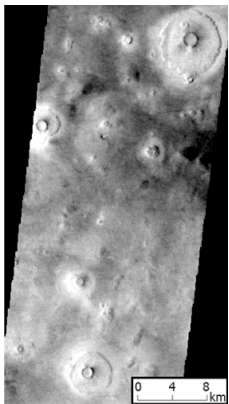


Fig. 1. Section of THEMIS VIS image V11743004 (78m/pxl) of a field of Pd craters. Image is centered at 56N, 84E. All Pd craters visible have diameters <2 km. Note the circular platform of the craters and pedestal margins.

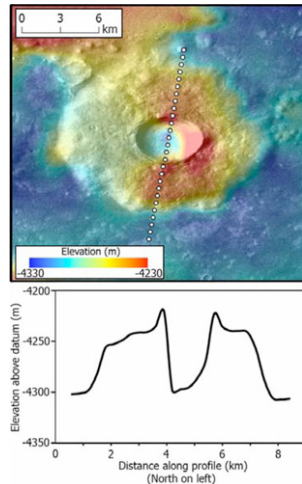


Fig. 2. THEMIS VIS image superposed on a MOLA elevation map showing a typical Pd crater and its pedestal plateau elevated above the surrounding terrain. The profile from MOLA data has a VE of ~36X.

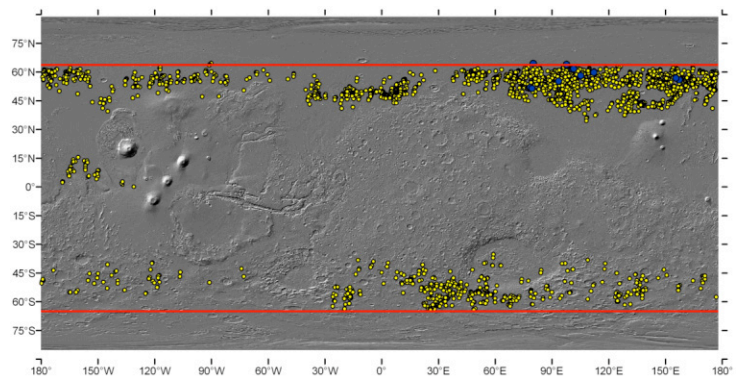


Fig. 3. Distribution of Pedestal (Pd) craters (yellow dots) and pitted-margin Pd craters in Utopia Planitia (blue dots) [24] between ~63°N and S.